19TH INTERNATIONAL COSMIC RAY CONFERENCE

LA JOLLA, USA AUGUST 11-23, 1985

CONFERENCE PAPERS

SH

SESSIONS VOL. 4

STUDY OF PHOTON EMISSION BY ELECTRON CAPTURE DURING SOLAR NUCLEI ACCELERATION: III. PHOTON PRODUCTION EVALUATIONS.

J. Pérez Peraza* and M. Alvarez*
Instituto de Goefísica, UNAM, 04510- C. U., México, D. F., MEXICO
A. Gallegos
UPICSA, 08400 - México, D. F., MEXICO

1. Introduction. Electromagnetic emission from the interaction of hydrogenic nuclei with atomic media has been widely studied in Laboratory. At astrophysical scale a similar scenario has been studied: high energy Cosmic Rays (bare nuclei)traversing a certain amount of interestellar matter while loosing energy by Coulomb interactions. Here we study to some extent the opposite scenario, in the sense that particle interaction and emission takes place as particles are being accelerated from the source thermal energies up to high energies. As particle sources we have chosen the Solar chromosphere and corona, where local ions are generally not bare nuclei, and there are often situations for which the amount of traversed matter is enough for the establishment of electron pick-up during acceleration, as was shown in paper SH 1.1-9. Here we limit our calculations to photon emission following electron capture and do not consider emissions following de-excitations. According to SH 1.1.-9 results electron capture is systematically established in atomic H conditions, but in ionized H it is established only at $T>2\times10^{6}$°K for nuclei of $Z>10$ and $E<30$ MeV/n; however, since σ_{cr} in ionized matter scales as Z_t= target atomic number, electron pick-up is established at $T>2\times10^{6}$°K when the contribution of heavy targets is considered. Actually, since the criteria for charge transfer establishment (SH 1.1-9) are practically independent of matter density, most of the electromagnetic emission expected here appears in this form. It should be noted that such criteria are limited in validity for the condition that the particle flight time within the acceleration volume be enough long for the amoung of traversed matter (X) be higher than the corresponding mean free path (λ) of the charge transfer process ($\rho v t > M/\sigma$): it can be seen that given a density (ρ) and particle velocity (v), since the cross-section (σ) decreases with T, the behavior of the time (t) is fundamental in determining whether ($X>\lambda$) or not. This can be tested from the employed acceleration time $t_f=[2/(2\mu c^2)^{0.5}\alpha_f](E^{\frac{1}{2}}-E_{th}^{\frac{1}{2}})$ in the Fermi process, and the betatron acceleration time $t_b=(1/2\alpha_b)\ell_n(E/E_{th})$, where E_{th} is the thermal energy per nucleon of the accelerated ions. For the evaluation of the acceleration efficiencies we recurred to the results of the criteria (α_f/α_c), (α_b/α_c) in SH 1.1-9, such that α_f=(criterium value) α_c(fermi), α_b=(criterium value) α_c (betatron). The general tendency in ionized matter is the increase of the acceleration time with T because α_c decreases with T, so, the above inequality is satisfied easily while the higher T. In atomic matter t_f decreases with T because α_c(Fermi) is T-independent, but the electron capture cross-section increases with T, as we shown in SH 1.1-8, so the inequality is satisfied. With betatron, t_b increases slowly with T as α_c(betatron) decreases with T, however, conditions are such that the inequality is systematically conserved. Similarly, though the electron loss cross-section decreases with T, as t_f does, much of conditions satisfy that inegality. Therefore, even if the density is very low the inegality is conserved because α_c decreases with density and the acceleration times becomes proportionally longer.

2. Method for Photon Production Evaluation. Once we have determined the energy range where electron capture is established, we know the initial charge state q^*_i at the corresponding lower energy value according to the normalization describen in SH 1.1-8 of the effective charge for charge equilibrium to the thermal charge state, when charge equilibrium was established at that particle energy level, or, the arbitrary expresion q^*_c for pure capture given in SH 1.1-9 (if electron loss does not establish). If electron capture begins from thermal energies $q^*_i = Q_L$. Since acceleration is

increasing particle energy, we test at each energy value whether $q_i^*-q_c^*\geq 1$ if charge equilibrium is established, or, $Q_L-q_c^*\geq 1$ if only pure electron loss is established; if not, we iterate to the next energy value with the corresponding q_i^* and q_c^* values in the former case, or $Q_L-q_c^*$, with q_c^* evaluated at the new energy in the 2nd case. When we find that an electron is captured, we evaluate the number of electrons retained by the ion $N_e=Z-q_c^*$. Furhter, we fit this number to the degeneracy condition $2n^2$: if the n-orbit is not still filled, we begin calculating orbit radius $r_n=n^2\hbar^2/Ze^2m_e$ [but, if it is filled we begin to evaluate orbit radius from (n+1)] in order to compare them with the capture radius ($r_c=q^*e^2/m_eV_R^2$), and in this way to determine at which energy level the electron will be captured; if $r_{n+i}<r_c<r_{n+i+1}$ we infer that the capture orbit is at $r_{n+i}=r_f$. When $r_c<r_n$ (n=1), we recur to the Sommerfeld eliptic orbits $r_\kappa=\kappa n\ ^2/m_eZ_e^2$, where κ is the quantic number determining the angular moment, and so, we proceed the evaluation from κ=n-1 till κ=1. In the cases that $r_c<r_\kappa(\kappa=1)$ we fall in the domain of relativistic mechanics that we have not studied in this preliminar work: this is the case at $T>5\times10^7$°K, when V_R becomes extremely high. Therefore, at each energy value we imposed 3 conditions for making possible the evolution of photon emission: (1) electron capture is established, (2) we find $q_c^*\leq q_i^*-1$ (3) $r_c\geq r_\kappa(\kappa=1)$. Once these conditions are remplished we evaluate the photon energy $h\nu=E(r_c)-E(r_f)\sim q^*e^2/r_f-q^*e^2/r_c$, and the photon flux at 1. A.U., $F/n_t=N(E)\sigma_c/4\pi R^2$ (photons/eV st/target atom). For our calculations we took the energy spectrum of protons demodulated for interplanetary propagation of the 4-VIII-72 event [1], $N(E)=8\times10^{35}\ E^{-3}$, and typical solar particle abundances [2], such that under the assumption $(O/H)_0=0.77\%$ we built the heavy ions spectra. For radiative capture we did not evaluate photon emission from electron braking as we have done in the case of Coulomb capture.

3. Results and Discussions. As is shown in the next series of pictures, our results are widely assorted depending on T, Z_t, Z, N(E, Z) and the acceleration process. The general tendencies show a frecuency drift toward high photon energies as particles increase their energy during acceleration, because $h\nu\sim 1/r_c$ and $r_c\sim 1/V_R$: oscilations are due to charge changes and the separation between r_c and the quantic level at r_f which is very sensitive to V_R. Typical drifts in atomic matter produces continum radiation from IR to X-ray (10^{-3} - 5×10^3)eV in $\Delta t\sim 1$s, whereas in ionized matter we obtained emission lines from UV to X-rays (50 eV-6.2KeV), with a finite width covered in $\Delta t\leq 0.5$s. It can be appreciated on the drift figures ($h\nu$-E) that the heavy the projectil the emission drifts to higher energies, because $h\nu\sim q^*/r_c^2\sim Z^2$. The range of energy drift widens with T, because the particle energy range for electron capture increases with T. Also the photon energy increase with T because the increase of V_R with T, but with oscilations due to the V_R-sensivity of the separation between r_c and the nearest orbit r_f. On the figures of energy spectra (Flux-$h\nu$) it can be noted that the heavier the target and the projectil the higher the intensity of the emission spectrrum. This follows from the fact that $F/n_t\sim\sigma_c N(E, Z)$ and σ_c increases with Z and Z_t. However, this tendency may also show oscilations because N(E, Z) does not increase always monotonically with Z. Also, the emission intensity increases with T in atomic matter and decreases with T in ionized matter, because the corresponding σ_c increases and decreases with T respectively. Photon fluxes in atomic and ionized matter are in the range 10^{-7}-10^7 ph./eVst/target-atom and 10^{-12}-10^8ph./eVst/target-atom. On the time profiles figures (Flux - t) the t-axis refers to t_f and t_b,

which are increasing functions of particle energy E. Since N(E, Z) is a decreasing function with E, therefore, phothon fluxes decrease with time during acceleration. Photon emission begins faster after acceleration onset with Fermi than with betatron acceleration, and more faster, in atomic than in ionized media, since acceleration efficiencies are higher in atomic matter: for instance, with Fermi acceleration begins $(10^{-5}-10^{-3})$s after acceleration onset, while with betatron begins $(10^{-3}-10^{-2})$s after acceleration onset, whereas in ionized matter corresponding time delays are (0.5-3.5)s and $\sim$ 2.3s respectively. From the values $\alpha_f \sim (4\times10^{-3}-10^{4})s^{-1}$ and $\alpha_b \sim (3.5 \sim 10^{5})s^{-1}$ in atomic matter, it is realized that acceleration from thermal energies in deep chromospheric layers is restricted to extremely constrained conditions of strong turbulence with extremely short length scales and very high magnetic field gradients, that might only occur in association with fast magnetic field annhilation in active neutral current sheets. On the other hand $\alpha_f \sim (3\times10^{-2} - 0.2)s^{-1}$, $\alpha_b \sim 2.4s^{-1}$ in coronal ionized matter is quite reasonable.

4. Conclusions. We have evaluated lower limits of photon fluxes from electron capture during acceleration in solar flares, because the arbitrary q_c^* assumed in this work evolves very slow with velocity, probably much more slowly than the physical actual situation: in fact, more emission is expected toward the IR region. Nevertheless, we claim to have shown the factibility of sounding acceleration processes, charge-evolution processes and physical parameters of the source itself, by the observational analysis of this kind of emissions. For instance, it would be interesting to search observationallly, for the predicted flux and energy drift of F_e ions interacting with the atomic O and F_e of the source matter, or, even more feasible for the X-ray lines at 4.2 KeV and 2.624 + 0.003 KeV from Fe and S ions in ionized Fe at T = 10^7°K respectively, the 418 $\pm$ 2 eV and 20 $\pm$ 4 eV lines of Fe and S in ionized Fe at 5×10^6°K, which are predicted from Fermi acceleration.

References

[1] Miroshnichenko, L. I. and Petrov, V. M., "Dynamics of Radiation Conditions in Space", Energoatomizdat, Moscow, 1985.

[2] Dietrich, W. F. and Simpson, J. A., Ap. J. 225, L41, 1978.

*On leave for the INAOE, Tonanzintla A.P. 51, 72000-Puebla,MEXICO.

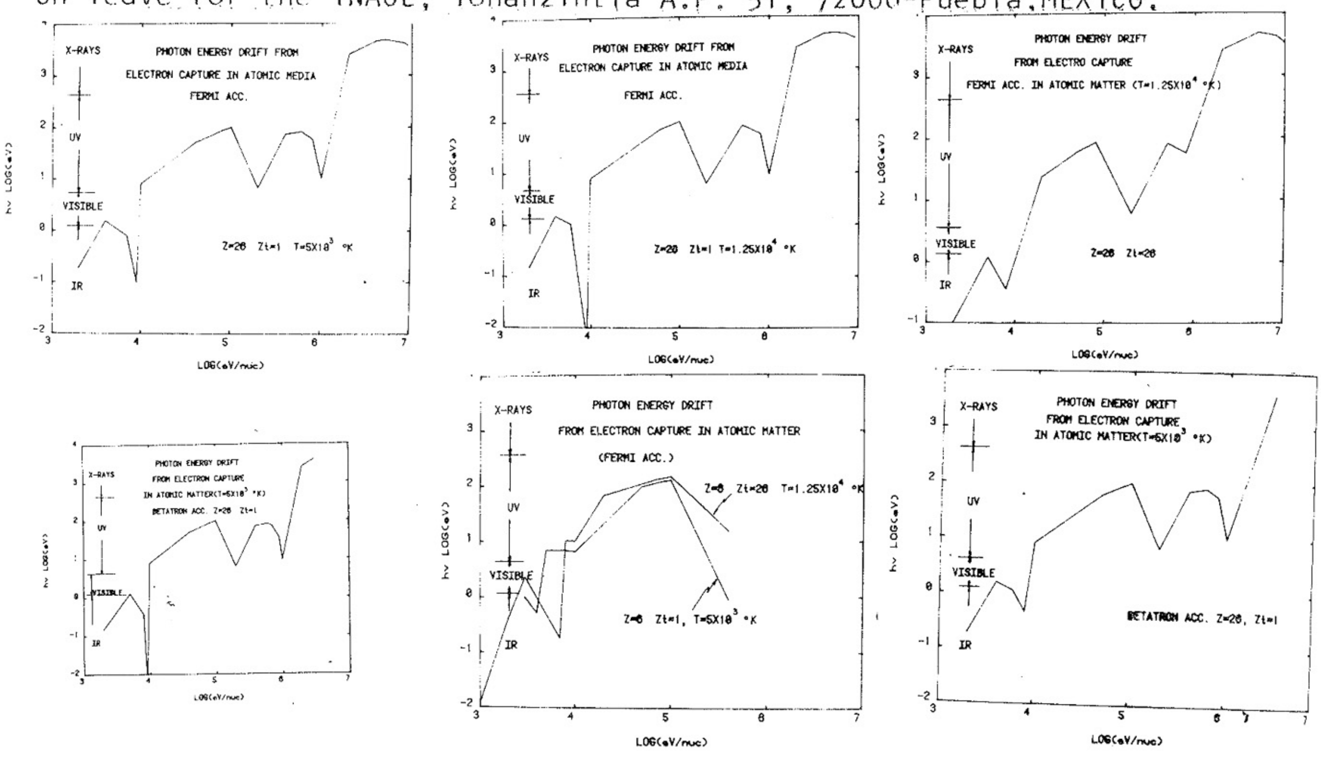

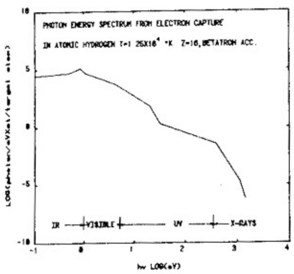
PHOTON ENERGY SPECTRUM FROM ELECTRON CAPTURE
IN ATOMIC HYDROGEN T=1.25X10⁴ °K Z=16,BETATRON ACC.
IR
VISIBLE
UV
X-RAYS
hν LOG(eV)
LOG(photon/eVxsl/target atom)

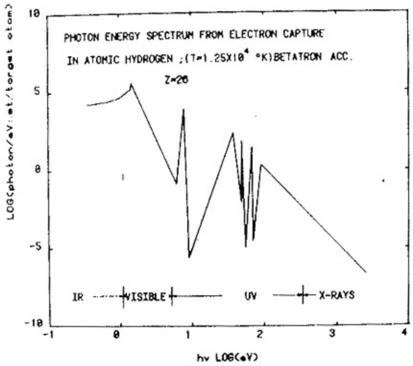
PHOTON ENERGY SPECTRUM FROM ELECTRON CAPTURE
IN ATOMIC HYDROGEN ;(T=1.25X10⁴ °K)BETATRON ACC.
Z=26
IR
VISIBLE
UV
X-RAYS
hν LOG(eV)
LOG(photon/eV/sl/target atom)

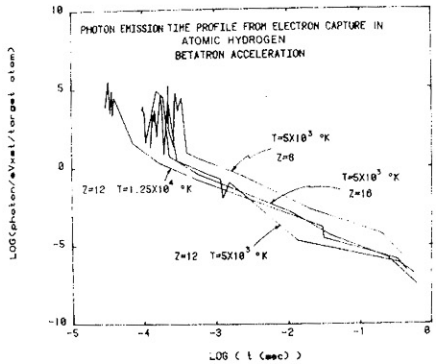
PHOTON EMISSION TIME PROFILE FROM ELECTRON CAPTURE IN
ATOMIC HYDROGEN
BETATRON ACCELERATION
T=5X10³ °K
Z=6
T=5X10³ °K
Z=16
Z=12 T=1.25X10⁴ °K
Z=12 T=5X10³ °K
LOG (t (sec))
LOG(photon/eVxsl/target atom)

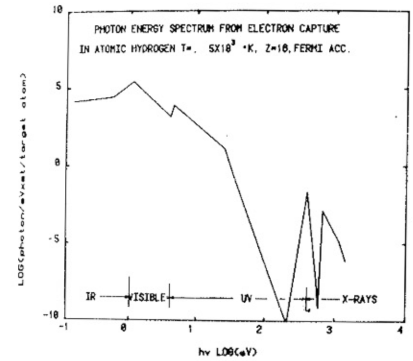
PHOTON ENERGY SPECTRUM FROM ELECTRON CAPTURE
IN ATOMIC HYDROGEN T= 5X10³ °K, Z=16,FERMI ACC.
IR
VISIBLE
UV
X-RAYS
hν LOG(eV)
LOG(photon/eVxsl/target atom)

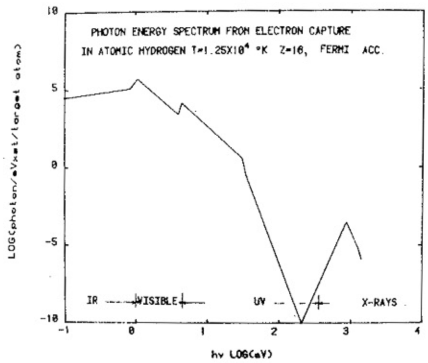
PHOTON ENERGY SPECTRUM FROM ELECTRON CAPTURE
IN ATOMIC HYDROGEN T=1.25X10⁴ °K Z=16, FERMI ACC.
IR
VISIBLE
UV
X-RAYS
hν LOG(eV)
LOG(photon/eVxsl/target atom)

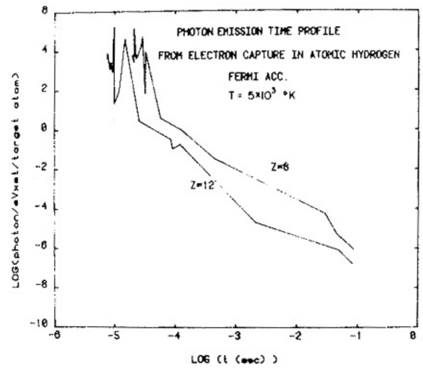
PHOTON EMISSION TIME PROFILE
FROM ELECTRON CAPTURE IN ATOMIC HYDROGEN
FERMI ACC.
T= 5X10³ °K
Z=6
Z=12
LOG (t (sec))
LOG(photon/eVxsl/target atom)

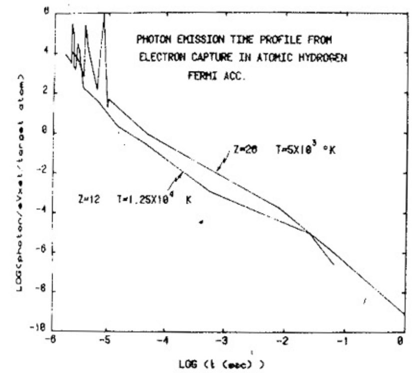
PHOTON EMISSION TIME PROFILE FROM
ELECTRON CAPTURE IN ATOMIC HYDROGEN
FERMI ACC.
Z=26 T=5X10³ °K
Z=12 T=1.25X10⁴ K
LOG (t (sec))
LOG(photon/eVxsl/target atom)

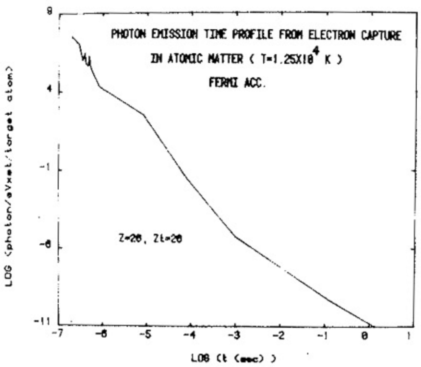
PHOTON EMISSION TIME PROFILE FROM ELECTRON CAPTURE
IN ATOMIC MATTER (T=1.25X10⁴ K)
FERMI ACC.
Z=26, Zt=26
LOG (t (sec))
LOG (photon/eVxsl/target atom)

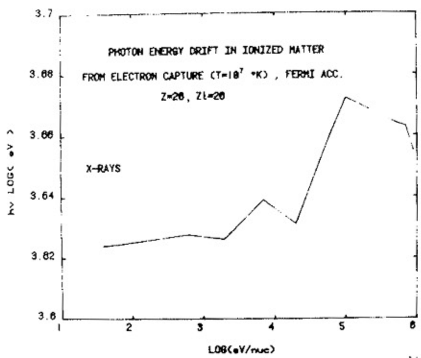
PHOTON ENERGY DRIFT IN IONIZED MATTER
FROM ELECTRON CAPTURE (T=10⁷ °K) , FERMI ACC.
Z=26, Zt=26
X-RAYS
LOG(eV/nuc)
hν LOG(eV)

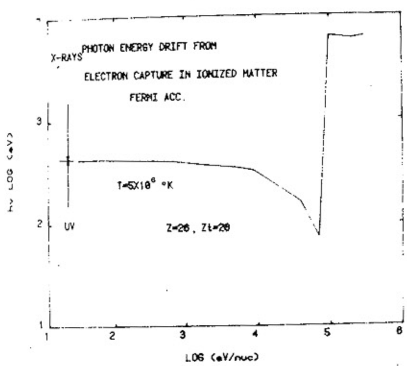
PHOTON ENERGY DRIFT FROM
ELECTRON CAPTURE IN IONIZED MATTER
FERMI ACC.
X-RAYS
T=5X10⁶ °K
UV
Z=26 , Zt=26
LOG (eV/nuc)
hν LOG (eV)

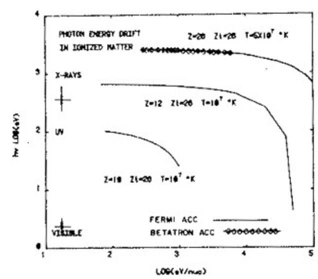
PHOTON ENERGY DRIFT
IN IONIZED MATTER
Z=26 Zt=26 T=5X10⁷ °K
X-RAYS
Z=12 Zt=26 T=10⁷ °K
UV
Z=16 Zt=26 T=10⁷ °K
FERMI ACC
BETATRON ACC
VISIBLE
LOG(eV/nuc)
hν LOG(eV)

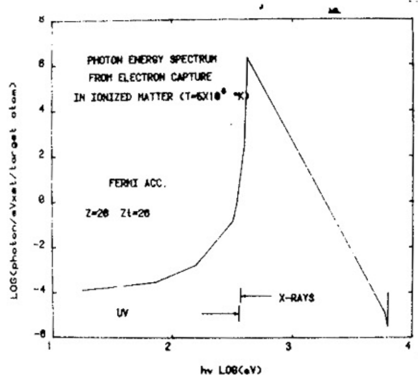
PHOTON ENERGY SPECTRUM
FROM ELECTRON CAPTURE
IN IONIZED MATTER (T=5X10⁶ °K)
FERMI ACC.
Z=26 Zt=26
X-RAYS
UV
hν LOG(eV)
LOG(photon/eVxsl/target atom)

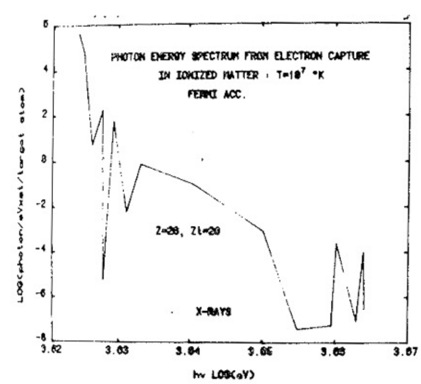
PHOTON ENERGY SPECTRUM FROM ELECTRON CAPTURE
IN IONIZED MATTER , T=10⁷ °K
FERMI ACC.
Z=26, Zt=26
X-RAYS
hν LOG(eV)
LOG(photon/eVxsl/target atom)

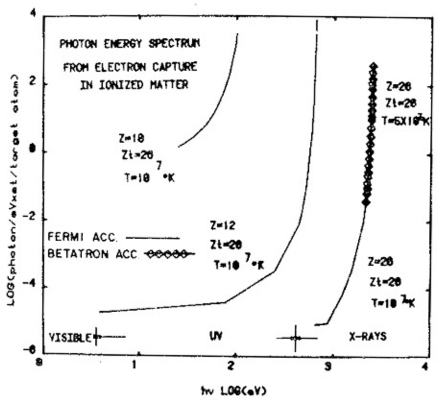
PHOTON ENERGY SPECTRUM
FROM ELECTRON CAPTURE
IN IONIZED MATTER
Z=16
Zt=26
T=10⁷ °K
Z=26
Zt=26
T=5X10⁷K
FERMI ACC.
BETATRON ACC
Z=12
Zt=26
T=10⁷ °K
Z=26
Zt=26
T=10⁷K
VISIBLE
UV
X-RAYS
hν LOG(eV)
LOG(photon/eVxsl/target atom)

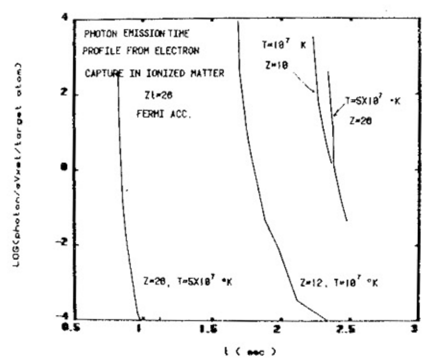
PHOTON EMISSION TIME
PROFILE FROM ELECTRON
CAPTURE IN IONIZED MATTER
Zt=26
FERMI ACC.
T=10⁷ K
Z=16
T=5X10⁷ °K
Z=26
Z=26, T=5X10⁷ °K
Z=12, T=10⁷ °K
t (sec)
LOG(photon/eVxsl/target atom)